*Biochimica et Biophysica Acta*, 981 (1989) 243–253
Elsevier



BBA 74419

# Behavior of spin labels in a variety of interdigitated lipid bilayers

J.M. Boggs [1], G. Rangaraj [1] and A. Watts [2]

[1] *Department of Clinical Biochemistry, University of Toronto, and Department of Biochemistry, Hospital for Sick Children, Toronto (Canada) and* [2] *Department of Biochemistry, University of Oxford, Oxford (U.K.)*

(Received 14 November 1988)
(Revised manuscript received 21 February 1989)

Key words: Spin label; Lipid bilayer; Interdigitated bilayer

**The behavior of a number of spin labels in several lipid bilayers, shown by X-ray diffraction to be interdigitated, has been compared in order to evaluate the ability of the spin label technique to detect and diagnose the structure of lipid bilayers. The main difference between interdigitated and non-interdigitated gel phase bilayers which can be exploited for determination of their structure using spin labels, is that the former have a much less steep fluidity gradient. Thus long chain spin labels with the nitroxide group near the terminal methyl of the chain, such as 16-doxylstearic acid, its methyl ester, or a phosphatidylglycerol spin label containing 16-doxylstearic acid (PG-SL), are more motionally restricted and/or ordered in the interdigitated bilayer than in the non-interdigitated bilayer. This difference is large enough to be of diagnostic value for all three spin labels in the interdigitated bilayers of dipalmitoylphosphatidylcholine/glycerol, dipalmitoylphosphatidylglycerol/polymyxin B, and the asymmetric 1-stearoyl-2-caproylphosphatidylcholine. A difference can also be detected for all three spin labels in the interdigitated bilayers of dihexadecylphosphatidylcholine, dipalmitoylphosphatidylcholine/ethanol, and 1,3-dipalmitoylphosphatidylcholine. However, it is not large enough to be of diagnostic value at low temperatures. Use of probes with the nitroxide group closer to the apolar/polar interface reveals that these latter interdigitated bilayers are more disordered or less closely packed. As the temperature is increased, however, the motion of the PG-SL does not increase as much in these interdigitated bilayers as in non-interdigitated bilayers. The difference in the motion and/or order of PG-SL between interdigitated and non-interdigitated bilayers is large enough at higher temperatures to be of value in diagnosing the structure of the bilayers. Thus by choice of a suitable spin label and a suitable temperature, this technique should prove useful for detection and diagnosis of lipid bilayer structure with a good degree of reliability. Caution must, of course be exercised, as with any spectroscopic technique. Spin labels will also be invaluable for more detailed studies of known interdigitated bilayers, which would be time- and material-consuming, if carried out using X-ray diffraction solely.**

## Introduction

Until recently it was believed that two-chain lipids always formed non-interdigitated bilayers in which the fatty acid chains of lipid molecules on opposite sides of the bilayer are packed end to end. However, it is now known that a number of lipids can form fully interdigitated bilayers in the gel phase, either by themselves [1,2], or in the presence of amphipathic substances such as proteins and polymers [3,4], drugs and similar small molecules [5–10], Tris buffer [11], monovalent salts [12], and when under high pressure [13]. Asymmetric chain length lipids can also form partially interdigitated or mixed (triple chain) interdigitated bilayers in the absence of added agents [14–21]. Interdigitation can be detected by X-ray [1,2,4–12,14,15,17,19,20] or neutron diffraction [13], since it results in a concomitant decrease in bilayer thickness and increase in the bilayer surface area per head group, as established in two fundamental X-ray diffraction studies [22,23]. However, it is useful to also be able to detect and/or diagnose the interdigitated bilayer by spectroscopic techniques, particularly if they are faster and require less sample than

Abbreviations: 1,2-DPPC, 1,2-dipalmitoyl-*sn*-glycero-3-phosphocholine; 1,3-DPPC, 1,3-dipalmitoyl-*sn*-glycero-2-phosphocholine; DHPC, 1,2-di-*O*-hexadecyl-*sn*-glycero-3-phosphocholine; 18 : 10PC, 1-stearoyl-2-caproyl-*sn*-glycero-3-phosphocholine; DPPG, 1,2-dipalmitoyl-*sn*-glycero-3-phosphoglycerol; PC, phosphatidylcholine; PMB, polymyxin B; 16-S-SL, 16-doxylstearic acid where doxyl stands for the 4′,4′-dimethyl-oxazolidine-*N*-oxyl derivative of the parent ketone; 5-S-SL, 5-doxylstearic acid; 16-MeS-SL, methyl ester of 16-S-SL; PG-SL, 1-palmitoyl-2-(16-doxyl-stearoyl)-*sn*-glycero-3-phosphoglycerol; H-TEMPO, 4-(*N*,*N*-dimethyl-*N*-hexadecyl)ammonium-2,2,6,6-tetramethylpiperidine-1-oxyl iodide.

Correspondence: J.M. Boggs, Department of Biochemistry, Hospital for Sick Children, 555 University Ave., Toronto, Ontario, Canada M5G 1X8.

X-ray diffraction. Unlike scattering techniques, spectroscopic techniques can also be used to study the dynamic properties of interdigitated bilayers and in some cases, to quantitate the percentage of lipid which is interdigitated. Interdigitated bilayers have been detected and studied by use of spin labels [3,21,24–26], Raman spectroscopy [16,27–29], high pressure infrared spectroscopy [30,31], and DPH fluorescence [32], although the diagnostic capability of these techniques has not been established.

Fatty acid or lipid spin labels with the spin label moiety near the terminal methyl of the acyl chain have been used to detect the fully interdigitated bilayers of dipalmitoylphosphatidylcholine (DPPC) in the presence of glycerol [24], dipalmitoylphosphatidylglycerol (DPPG) in the presence of polymyxin B (PMB) [24,26], and the mixed interdigitated bilayer formed by asymmetric forms of phosphatidylcholine, such as 1-stearoyl-2-caproylphosphatidylcholine (18 : 10PC) [25]. These spin labels are much more motionally restricted and/or ordered in the interdigitated bilayer than in the non-interdigitated bilayer. Indeed the motion and/or order become similar to that of a spin label bound much closer to the carboxyl group of a fatty acid. Thus the fluidity gradient, found in non-interdigitated bilayers even in the gel phase [33,34], is abolished or much less steep in the interdigitated bilayer. At low temperatures, the spectrum resembles the easily recognizable powder spectrum. This degree of motional restriction has not been reported to occur in non-interdigitated bilayers except in the presence of intrinsic proteins; in that case it also occurs in the liquid-crystalline phase [35]. This unusual behavior coupled with the magnitude of the effect on the spin label motion suggest that this technique may be capable of diagnosing interdigitated bilayers, if intrinsic proteins are not present and if used with caution. Results obtained with these spin labels in DPPG in the presence of the extrinsic and amphipathic protein, myelin basic protein, and in highly asymmetric forms of cerebroside sulfate have led to the prediction that these also form interdigitated bilayers under some conditions [3,21]. This technique can also be used to quantitate the percentage interdigitated lipid in mixtures of lipids from the amount of spin label which is motionally restricted (Wang, H-Y., Boggs, J.M. and Tümmler, B., unpublished data).

In the present study we examine the behavior of several long hydrocarbon chain spin labels in three additional bilayer systems, which were shown by others to be interdigitated using X-ray diffraction, in order to further evaluate the diagnostic capability of this technique and to characterize the molecular organization in these systems. These interdigitated systems include 1,3-DPPC [1], DHPC [2], and 1,2-DPPC in the presence of high concentrations of ethanol [10]. They are compared to several interdigitated bilayer systems studied previously, DPPG-PMB complexes, DPPC in the presence of glycerol, and 18 : 10PC.

## Materials and Methods

The phospholipids, 1,2-di-*O*-hexadecyl-sn-glycero-3-phosphocholine (DHPC) and 1,3-dipalmitoyl-*sn*-glycero-2-phosphocholine (1,3-DPPC) were purchased from Calbiochem-Behring Corp. (La Jolla, CA), 1,2-dipalmitoyl-*sn*-glycero-3-phosphocholine (1,2-DPPC) from Sigma Chemical Co. (St. Louis, MO), 1,2-dipalmitoyl-*sn*-glycero-3-phosphoglycerol (DPPG) from Avanti Polar Lipids (Birmingham, AL), and 1-stearoyl-2-caproyl-*sn*-glycero-3-phosphocholine (18 : 10PC) was a generous gift from Dr. J.T. Mason. The spin labels, 16-doxylstearic acid (16-S-SL), 5-doxylstearic acid (5-S-SL), and the methyl ester of 16-doxylstearic acid (16-MeS-SL) were purchased from Syva (Palo Alto, CA), 4-(*N*,*N*-dimethyl-*N*-hexadecyl)ammonium-2,2,6,6-tetramethylpiperidine-1-oxyl iodide (H-TEMPO) from Molecular Probes (Eugene, OR), and a phosphatidylglycerol spin label, 1-palmitoyl-2-(16-doxylstearoyl)-*sn*-glycero-3-phosphoglycerol (PG-SL) was synthesized as described [45]. Polymyxin B sulfate (PMB) was from Sigma Chemical Co. (St. Louis, MO), 100% ethanol from Consolidated Alcohols (Toronto, Canada), and glycerol from Fisher Scientific (Nipean, Ont., Canada).

The required lipids and spin label were combined in chloroform/methanol solutions of the lipid and spin label. In the case of PMB, a chloroform/methanol solution of the drug was also combined with the lipid and spin label at a mole ratio of PMB to DPPG of 1 : 5. After evaporation of the solvent under a stream of nitrogen, the sample was evacuated in a lyophilizer at about 0.1 Torr for 2 h). The required liquid, either buffer, distilled water, 100% glycerol, or ethanol solutions made up in distilled water, was added. The buffer, which was used only for the PMB sample, was 2 mM Hepes containing 0.1 M NaCl at pH 7.4. All samples were dispersed by vigorous vortex mixing at a temperature above the lipid phase transition temperature. In the case of DHPC, the sample was also freeze-thawed and vortexed twice at 50 °C; this procedure was repeated once more. Samples with ethanol were prepared in capped tubes and incubated at 45 °C for 5 min after vortexing. The lipid to spin label mole ratio ranged from 200 : 1 to 100 : 1. The lipid concentration was 2 μmol/50 μl glycerol or 2 μmol/500 μl aqueous solution. The aqueous samples were divided in half and each half centrifuged in an Eppendorf centrifuge. For DSC measurements, most of the supernatant was removed and the wet pellet was loaded into an aluminum DSC pan. For ESR measurements, all but about 50 μl of supernatant was removed and the suspension was loaded into a 50 μl capillary tube. The capillary tube was sealed at one end with a torch and the tube

centrifuged at 2000 rpm. Glycerol samples were treated as described previously [24]. In order to study the subgel transition of 1,3-DPPC, the sample was stored in the freezer for at least 1 month.

For calorimetry experiments, samples were examined on a Perkin-Elmer DSC-2 equipped with a Perkin-Elmer data station. The temperatures of the subgel, premelt ($T_p$) and main gel to liquid-crystalline ($T_m$) phase transitions were measured as the temperatures of maximum heat absorption. At heating and cooling rates of 10 C°/min, the $T_m$ values on cooling are 4.5 C° less than on heating for a pure lipid, such as 1,2-DPPC, which has a rapidly reversible gel-to-liquid crystalline phase transition. This is considered to be instrumental hysteresis and decreases to 0.7 C° at slower heating and cooling rates of 1.25 C°/min. Any difference greater than these is assumed to be true hysteresis in the phase behavior. Similar differences in $T_m$ values on heating and cooling to those shown in Table II at 1.25 C°/min were found at heating and cooling rates of 10 C°/min.

ESR spectra were measured on a Varian E-104B spectrometer equipped with a Varian temperature controller and a DEC LSI-11 based microcomputer system. All samples were heated to a temperature above the phase transition temperature just before measuring the spectra in the gel phase, unless, as for 1,3-DPPC, the spectrum of the subgel phase was to measured. The maximum hyperfine splitting, $2T_{max}$, of the ESR spectra, measured as shown in Fig. 2C, was used as a measure of the degree of order and/or motional restriction of the probe in the lipids below their gel to liquid-crystalline phase transition temperatures [47].

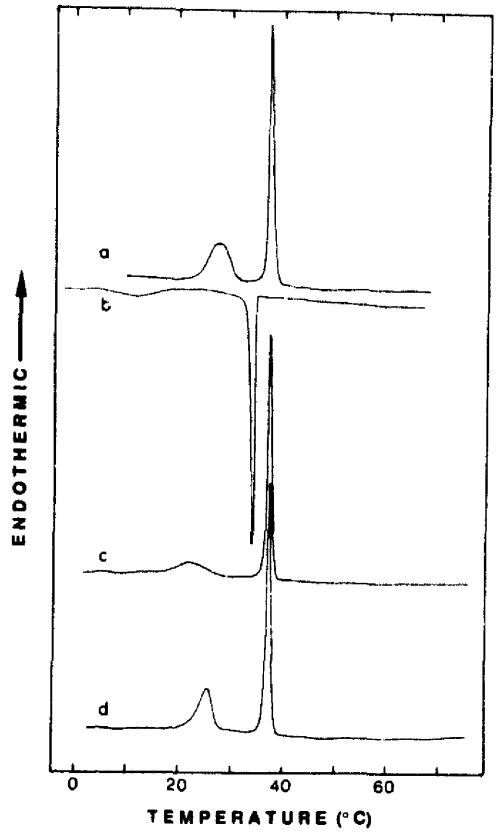


Fig. 1. DSC thermograms of 1,3-DPPC at heating and cooling rates of 5 C°/min. (a) First heating scan after storage at −20°C for 4 weeks; (b) cooling scan; (c) reheating scan after fast cooling at 20–40 C°/min; and (d) reheating scan after cooling to 14°C, incubating at that temperature for 30 min, then cooling further to −3°C, and immediately reheating. All heating scans were started from −3°C. Sensitivity setting for all scans was 0.8 mcal/s. Instrumental hysteresis between heating and cooling scans is 3.5 C° at heating and cooling rates of 5 C°/min.

## Results

### *1,3-DPPC*

An X-ray diffraction study [1] showed that if an aqueous dispersion of 1,3-DPPC is stored for a prolonged time at −3°C, the bilayers transform into a non-interdigitated crystalline subgel phase similar to that formed by 1,2-DPPC. In a transition centered at 27°C, the subgel phase of 1,3-DPPC transforms into a gel phase, which was shown to be interdigitated; it undergoes a gel to liquid-crystalline phase transition at 37°C. If the sample is then cooled relatively rapidly, it does not revert to the subgel phase but to another gel phase which was thought to be non-interdigitated [1]. On reheating, this gel phase undergoes a low enthalpy transition which resembles a premelt transition, at a somewhat lower temperature than the subgel transition; the transition to the liquid-crystalline phase is unaffected. This behavior of 1,3-DPPC is shown in the DSC scans in Fig. 1a–c, resembling those in Ref. 1. In addition, we show that if the sample is cooled to 14°C (the temperature of the low enthalpy peak in Fig. 1b observed on cooling at 1.25 C°/min) and incubated at that temperature for 30 min, the subsequent heating scan (Fig. 1d) more closely resembles that on first heating (Fig. 1a), recorded on a sample after prolonged incubation at low temperature. The low enthalpy peak in Fig. 1d occurs at 25.7°C, in between those of 27°C and 22.7°C shown in Fig. 1a and 1c, respectively and the enthalpy is 80% of that observed in Fig. 1a for the transition at 27°C.

The spin label, 16-S-SL, was used to investigate the dynamic properties of the lipid in 1,3-DPPC bilayers and to determine if this probe is useful for diagnosis of interdigitation of this lipid. At low temperatures, before cycling through the phase transition, the spin label gives a spectrum with an exchange broadened spectral component as well as a spectral component resulting from free spin label in the aqueous phase, indicating that it phase separates into its own domain and goes into the aqueous phase. Thus it is not soluble in the subgel crystalline phase of 1,3-DPPC, as found earlier for subgel phases of other lipids [25]. At 32°C, in between

TABLE I

*Comparison of $T_{max}$ values (G) of spin labels in interdigitated and noninterdigitated lipid bilayers* [a]

| Lipid | Bilayer structure [b] | 16-S-SL | | PG-SL | | 16-Me-SL | | 5-S-SL | | H-TEMPO | |
|---|---|---|---|---|---|---|---|---|---|---|---|
| *Temperature* | | *4°C* | *32°C* | *4°C* | *32°C* | *4°C* | *32°C* | *4°C* | *32°C* | *4°C* | *32°C* |
| 1,2-DPPC | N | 25.2 | 20.5 | 28.7 | 20.5 | ~ 26 | 18.8 | 30.9 | 28.0 | 32.4 | 27.3 |
| 1,3-DPPC | I | 27.6 | 21.8 | 30.7 | 28.9 | 26.6 | 21.6 | 31.2 | 28.0 | 30.7 | 27.3 |
| 1-18,2-10-PC | I | 29.0 | | | | | | 30.9 | | 32.1 | |
| *Temperature* | | *9°C* | *22°C* | *9°C* | *22°C* | *9°C* | *22°C* | *9°C* | *22°C* | *9°C* | *22°C* |
| 1,2-DPPC | N | 22.3 | 21.0 | 28.2 | 23.4 | 22.3, 27.6 | 20 | 30.8 | 30 | 32.4 | 31.1 |
| DHPC | I | 24.8 | 21.9 | 28.7 | 22, 28.6 | 24.1 | 22.4 | 29.9 | 28.9 | 29.4 | 27.9 |
| 1,2-DPPC + 40 mg/ml ethanol | N | 21.9 | | 27.5 | 21.8 | | | 30.5 | | 32.0 | |
| 1,2-DPPC + 100 mg/ml ethanol | I | 23.2 | | 30.1 | 28.2 | | | 29.5 | | 30.9 | |
| DPPG | N | 24.1 | | 28.5 | 25.6 | 24.0 | | 30.2 | | 32.4 | |
| DPPG-PMB | I | 30.2 | | 31.5 | 30.4 | 30.7 | | 31.9 | | 32.9 | |
| 1,2-DPPC + glycerol | I | 31.4 | | | | 31.5 | | 31.9 | | 33.2 | |

[a] Temperature of measurement varies and is indicated in the columns of figures. The reproducibility and accuracy of measurement of the $T_{max}$ values is within ±0.2 G.

[b] As determined by X-ray diffraction. I, interdigitated; N, non-interdigitated.

the endothermic transitions shown in Fig. 1a, 16-S-SL is soluble in the interdigitated gel phase of the lipid and gives a spectrum characteristic of anisotropic motion, typical of gel phase bilayers. However, the $T_{max}$ value is only 1.3 G greater than that of the non-interdigitated bilayer of 1,2-DPPC at this temperature (Table I). Thus this spin label can detect a difference between the interdigitated and non-interdigitated bilayers at 32°C, but is not sufficiently motionally restricted in the interdigitated bilayer of 1,3-DPPC, when compared to 1,2-DPPC, to allow its structure to be determined if it were previously unknown.

In the phase formed during slow cooling the spin label again becomes insoluble, indicating that slow cooling allows transformation back into the subgel phase, as suggested by the DSC results. The change in the spectrum from one characteristic of anisotropic motion to one characteristic of exchange broadening occurs around 14°C, i.e., during the low enthalpy transition observed by DSC. Thus the subgel phase reforms during this transition, although it can also form more slowly at lower temperatures. If the sample is cooled rapidly to 4°C, however, the spin label remains soluble in the bilayer, indicating that the lipid is not in the subgel phase, but in a gel phase. The $T_{max}$ value of 16-S-SL in this gel phase is 27.6 G, 2.4 G greater than that in 1,2-DPPC (Table I). However, it is not as great as that found in interdigitated bilayers studied previously, which have $T_{max}$ values of at least 29 G at this low temperature [24,25]. A difference from 1,2-DPPC of only 2.4 G is probably not large enough to diagnose the structure of this gel phase.

In contrast, the spectrum of the lipid spin label, PG-SL, which contains the same nitroxide positional isomer, is considerably different when reporting from interdigitated bilayers of 1,3-DPPC at 32°C than from non-interdigitated bilayers of 1,2-DPPC as shown in Fig. 2A and B, respectively. At this temperature, the $T_{max}$ value is 28.9 G for 1,3-DPPC in contrast to a value of about 20 G for 1,2-DPPC (Table I). The difference is large enough at this temperature to be diagnostic of the structure of the interdigitated gel phase of 1,3-DPPC.

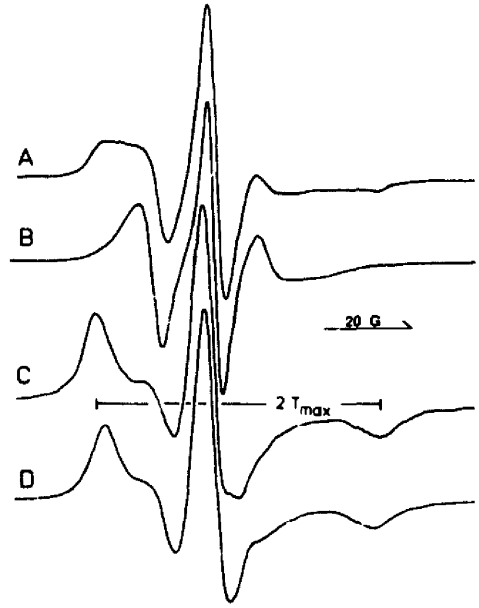


Fig. 2. ESR spectra of PG-SL in (A) 1,3-DPPC at 32°C; (B) 1,2-DPPC at 32°C; (C) 1,3-DPPC at 4°C; and (D) 1,2-DPPC at 4°C. Method of measurement of the spectral parameter, $2T_{max}$ is indicated in (C). All spectra are plotted normalized to the same center peak height. Both samples were heated to above their phase transition temperatures before measuring the spectra.

On cooling rapidly to 4°C, a powder type spectrum with $T_{max}$ of 30.7 G is obtained for PG-SL in 1,3-DPPC (Fig. 2C). At this low temperature, PG-SL is also relatively motionally restricted in 1,2-DPPC (Fig. 2D). However, the $T_{max}$ value is 2 G less than for 1,3-DPPC at this temperature (Table I) and the difference increases with increasing temperature. This motional restriction of PG-SL in 1,3-DPPC occurred at all temperatures up to the phase transition temperature and suggests that the gel phase formed after rapid cooling to 4°C is also interdigitated and is probably the same interdigitated gel phase shown by X-ray diffraction to form when the subgel phase undergoes its transition at 27°C in Fig. 1a. Thus the interdigitated gel to liquid-crystalline phase transition of this lipid is reversible and the interdigitated gel phase occurs at all temperatures below the phase transition temperature, until the subgel phase reforms during the transition at 14°C or after prolonged storage at a low temperature. Like 16-S-SL, PG-SL is insoluble in the subgel phase formed either after prolonged incubation at a low temperature or after slow cooling from the liquid-crystalline phase.

*DHPC*

DHPC molecules in bilayers have been shown by Ruocco et al. [2] to be interdigitated at all temperatures up to the premelt transition at 35°C. However, the $T_{max}$ value of the spectrum of 16-S-SL in this interdigitated bilayer at 9°C is only 2.5 G greater than for 1,2-DPPC (Table I). At 22°C the difference in $T_{max}$ of 16-S-SL between DHPC and 1,2-DPPC bilayers is even less. PG-SL has a much larger $T_{max}$ value in DHPC than 16-S-SL at these temperatures. However, at 9°C, there is little difference in $T_{max}$ of PG-SL between DHPC and 1,2-DPPC. At 14°C there are two components in the spectrum of PG-SL in DHPC (Fig. 3A) and only one, characteristic of relatively restricted motion, in 1,2-DPPC (Fig. 3B). One of the spectral components for PG-SL in DHPC at this temperature has a similar $T_{max}$ value as in 1,2-DPPC while the other has a lower value. On increasing the temperature further, however, the more motionally restricted spectral component for PG-SL is retained for DHPC as shown at 22°C in Fig. 3C, but not for 1,2-DPPC (Fig. 3D), allowing a significant difference between the two lipids to be detected.

The spectra of PG-SL in DHPC at 14°C and 22°C were resolved into their motionally restricted and more mobile components by subtracting appropriate amounts of each spectrum from the other, as shown in Fig. 3E and F. The $T_{max}$ value of the motionally restricted component in DHPC (Fig. 3E) is 28.6 G while that of 1,2-DPPC at 14°C is 28.1 G. The population of spin labels giving rise to the mobile spectral component in DHPC at 14°C (Fig. 3F) has lower order than the spin label in 1,2-DPPC at 22°C (Fig. 3D). Thus attempts to subtract the spectra in 1,2-DPPC from those in DHPC

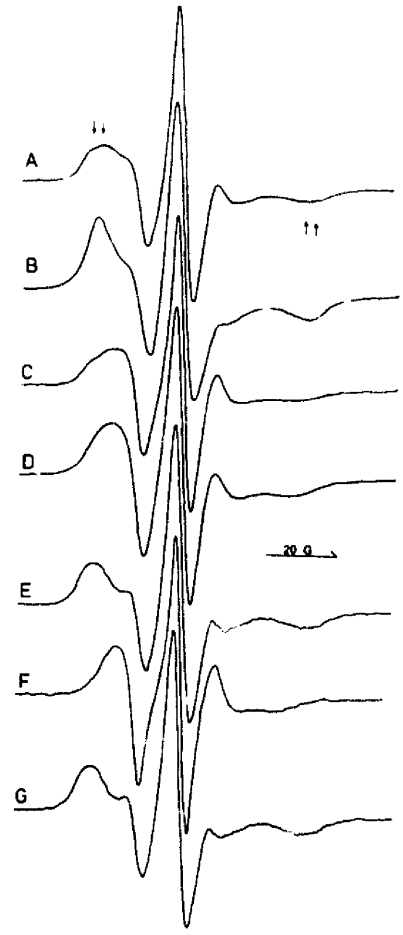


Fig. 3. ESR spectra of PG-SL in bilayers of (A) DHPC at 14°C; (B) 1,2-DPPC at 14°C; (C) DHPC at 22°C; (D) 1,2-DPPC at 22°C; (E) the motionally restricted component in the spectrum of DHPC at 14°C obtained by subtracting a fractional amount of the spectrum of DHPC at 22°C from that at 14°C; (F) the mobile component in the spectrum of DHPC at 22°C obtained by subtracting a fractional amount of the spectrum of DHPC at 14°C from that at 22°C; (G) the motionally restricted component in the spectrum of DHPC at 22°C, obtained by subtracting a fractional amount of the mobile component in (F) from the spectrum of DHPC at 22°C. The mobile and more motionally restricted components in the spectrum of DHPC in (A) are indicated by vertical arrows. These spectral components are relatively independent of temperature over this range, making these subtractions possible. The spectra shown are plotted normalized to the same center peak height. However, they were not normalized before subtraction. Both samples were heated to above their phase transition temperatures before measuring the spectra.

were not successful. The motionally restricted spectral component for PG-SL in DHPC at 22°C) was resolved by subtracting the mobile component in Fig. 3F from the spectrum shown in Fig. 3C. The result is shown in Fig. 3G and has a $T_{max}$ value of 28.6 G in contrast to a value of 23.4 G for 1,2-DPPC at 22°C (Table I). Thus the spectral parameters of PG-SL in DHPC are relatively independent of temperature over this range, in contrast to 1,2-DPPC. The more motionally restricted component in DHPC is retained up to 35°C, the tem-

perature of the premelt transition, where it then disappears leaving a spectrum resembling that of the non-interdigitated gel phase bilayer of 1,2-DPPC at this temperature.

The occurrence of two components in spectra of PG-SL in DHPC may indicate the presence of two populations of lipid with different molecular organization. Such behavior was not reported in a study of this lipid using X-ray diffraction [2]. Although Kim et al. [36] found in an X-ray diffraction study that at low water contents (< 32% water) DHPC forms a non-interdigitated bilayer, under conditions where it is fully hydrated, as used in this study, their results indicated that it was entirely interdigitated. However, Levin et al. [37] observed significant gel and liquid-crystalline phase polymorphism in DHPC even when fully hydrated. After repeated slow cycling through the phase transition, the Raman spectra of DHPC are more consistent with formation of an interdigitated bilayer. Similar treatment was found to have no effect on the ESR spectra of DHPC. If the more mobile component in ESR spectra of PG-SL in DHPC is indeed due to a population of non-interdigitated lipid, it indicates that at temperatures below the premelt transition, DHPC is more disordered than 1,2-DPPC in the center of the bilayer, when it is not interdigitated.

Alternatively, the presence of two components in the ESR spectra may indicate that the spin-labeled lipid intercalates into the interdigitated bilayer of this lipid in two different ways. Spectra of 16-S-SL in DHPC contained only one component. It is not obvious why PG-SL might do this, but a DHPC spin label might better monitor the organization of this lipid than a PG spin label. In any case, the significant difference in the spectra of DHPC and 1,2-DPPC at 22°C certainly reflects the difference between an interdigitated and a non-interdigitated bilayer structure and is large enough to be suggestive of interdigitation if the structure were unknown.

*DPPC in the presence of ethanol*

Simon and McIntosh [10] showed that at ethanol concentrations of 60 mg/ml or higher, 1,2-DPPC forms an interdigitated bilayer. Ethanol has a biphasic effect on the transition temperature of this lipid [38]. The concentration where interdigitation begins to occur is just above that at which the gel to liquid-crystalline phase transition temperature is at a minimum, and where it starts to increase [38]. At 40 mg/ml ethanol, where 1,2-DPPC forms a non-interdigitated bilayer, the $T_{max}$ value of 16-S-SL at 9°C is decreased relative to pure 1,2-DPPC (Table I), indicating that the non-interdigitated bilayer is disordered by this concentration of ethanol. At 100 mg/ml, where the bilayer is interdigitated, the $T_{max}$ value of 16-S-SL is 0.9 G greater than in pure 1,2-DPPC. This small but significant increase reflects the greater order of the interdigitated bilayer. However, it is not large enough to allow a prediction of the structure if it were unknown.

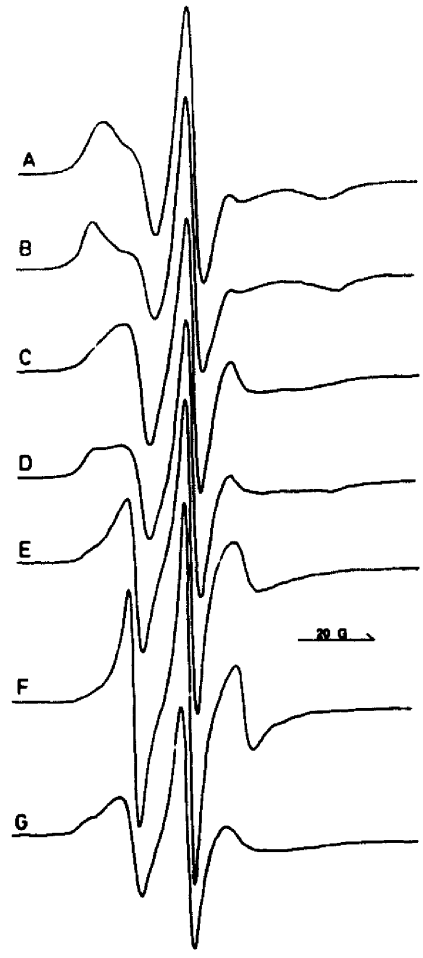


Fig. 4. ESR spectra of PG-SL in 1,2-DPPC (A) +40 mg/ml ethanol at 9°C; (B) +100 mg/ml ethanol at 9°C; (C) +40 mg/ml ethanol at 22°C; (D) +100 mg/ml ethanol at 22°C; (E) +100 mg/ml ethanol at 39°C on heating; (F) +100 mg/ml ethanol at 39°C on cooling from above the phase transition temperature, plotted at the same scale as (E); (G) +100 mg/ml ethanol at 34°C on cooling, plotted at the same scale as (E) and (F). Spectra in (A)–(D) are plotted normalized to the same center peak height.

At 9°C, these concentrations of ethanol have similar effects on the $T_{max}$ value of PG-SL as on 16-doxylstearic acid, although the actual values are greater for PG-SL (Table I, Fig. 4A, B). The difference in $T_{max}$ values of PG-SL in the non-interdigitated and interdigitated bilayers is probably not great enough at this temperature to be of diagnostic value. However, at 22°C there is a significant difference between the spectra of PG-SL in 1,2-DPPC at 40 and 100 mg/ml ethanol as shown in Fig. 4C, D, respectively. At 100 mg/ml ethanol most of the spin label is still motionally restricted, with a $T_{max}$ value of 28.2 G, while at 40 mg/ml, most of the spin label has much more motion with a $T_{max}$ value of 21.8 G (Table I). Thus the difference at this temperature is

TABLE II

*Effect of ethanol on transition temperatures of DPPC on heating and cooling*

At heating and cooling rates of 1.25 C°/min.

| Ethanol concentration (mg/ml) | Heat | | Cool [a] | |
|---|---|---|---|---|
| | $T_p$ (°C) | $T_m$ (°C) | $T_m$ (°C) | $\Delta T$ [a] (C°) |
| 0 | 34.1 | 41.2 | 40.5 | 0.7 |
| 40 | 28.2 | 39.7 | 39 | 0.7 |
| 100 | | 41.1 | 39, 40 [b] | 2.1, 1.1 [b] |
| 150 | | 41.9 | 39.1 | 2.8 |
| 200 | | 42.2 | 37.6 | 4.6 |

[a] $\Delta T$ is the difference in transition temperature observed on heating and cooling. Differences greater than 0.7 C° at a heating and cooling rate of 1.25 C°/min are attributed to hysteresis in the lipid behavior.

[b] Major peak is underlined.

large enough to predict that the bilayer is interdigitated. A significant amount of the motionally restricted component is retained in the 100 mg/ml sample up to the transition temperature as shown for the spectrum at 39°C in Fig. 4E. ESR spectra of the sample at 100 mg/ml at 39°C and 34°C, on cooling from above the phase transition temperature, are shown in Fig. 4F and G, plotted out on the same scale as that in Fig. 4E. The spectrum on cooling to 39°C (Fig. 4F) has less motionally restricted component than that in Fig. 4E, obtained after heating from a low temperature to 39°C. However, that obtained on cooling further to 34°C (Fig. 4G) has a significant amount of motionally restricted component, and is similar to that obtained at this temperature on heating (not shown). This indicates that interdigitation occurs on cooling, at a temperature close to the liquid-crystalline to gel phase transition temperature.

Using spectrophotometry, Rowe [39] showed that there is considerable hysteresis in the phase transition of 1,2-DPPC on heating and cooling at high ethanol concentrations, with the phase transition temperature on cooling several degrees below that on heating. We confirm this hysteresis using DSC as shown in Table II) and Fig. 5. In addition, we show that at 100 mg/ml the peak on cooling can be resolved into 2 peaks, about 1 degree apart, at slow cooling rates (Fig. 5C). At a higher concentration, 200 mg/ml, only one transition is seen on cooling at an even lower temperature (Table II). The hysteresis in the phase behavior at high ethanol concentrations suggests that the lipid may freeze initially into a non-interdigitated bilayer, which is less stable relative to the liquid-crystalline phase than the interdigitated bilayer. Therefore, the higher temperature transition seen at 100 mg/ml by DSC on cooling in Fig. 5C may be due to formation of an interdigitated bilayer while the lower temperature transition may be due to freezing of some of the lipid into a non-interdigitated bilayer. At 200 mg/ml all of the lipid may freeze initially into a non-interdigitated bilayer. It may then become interdigitated at a lower temperature.

*Behavior of other spin labels in interdigitated bilayers*

The behavior of a number of other spin labels in several interdigitated systems is also compared in Table I. We showed previously that 16-S-SL is motionally restricted at low temperatures, giving a $T_{max}$ value of around 31 G, in the interdigitated bilayers of DPPG/PMB and 1,2-DPPC/glycerol [24] and 29 G in 18:10PC [25] in contrast to the interdigitated DHPC, 1,2-DPPC, and 1,2-DPPC/ethanol systems studied here. The methyl ester of 16-doxylstearic acid (16-MeS-SL) is

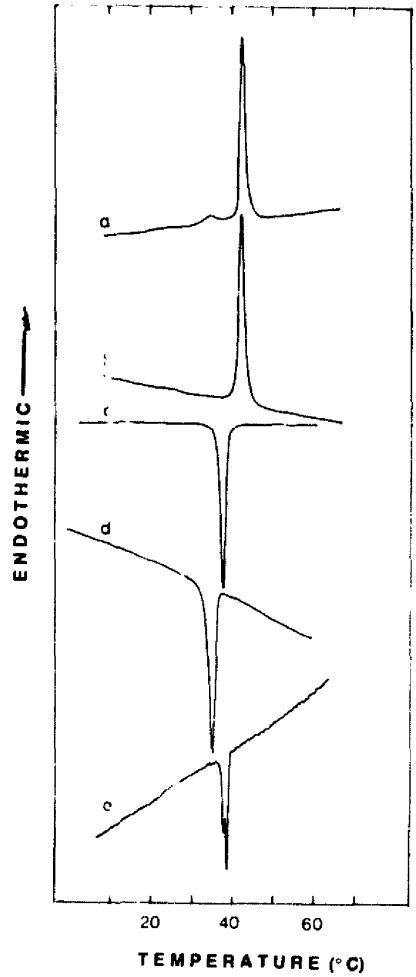


Fig. 5. DSC thermograms of (a) 1,2-DPPC, heating scan at 10 C°/min; (b) 1,2-DPPC + 100 mg/ml ethanol, heating scan at 10 C°/min; (c) 1,2-DPPC, cooling scan at 10 C°/min; (d) 1,2-DPPC + 100 mg/ml ethanol, cooling scan at 10 C°/min; and (e) 1,2-DPPC + 100 mg/ml ethanol, cooling scan at 1.25 C°/min. Different amounts of lipid were present in the DSC pans for the two samples in the presence and absence of ethanol so the peak areas cannot be directly compared. Sensitivity setting in mcal/s were (a, c) 1.5; (b, d) 1.0; (e) 0.3.

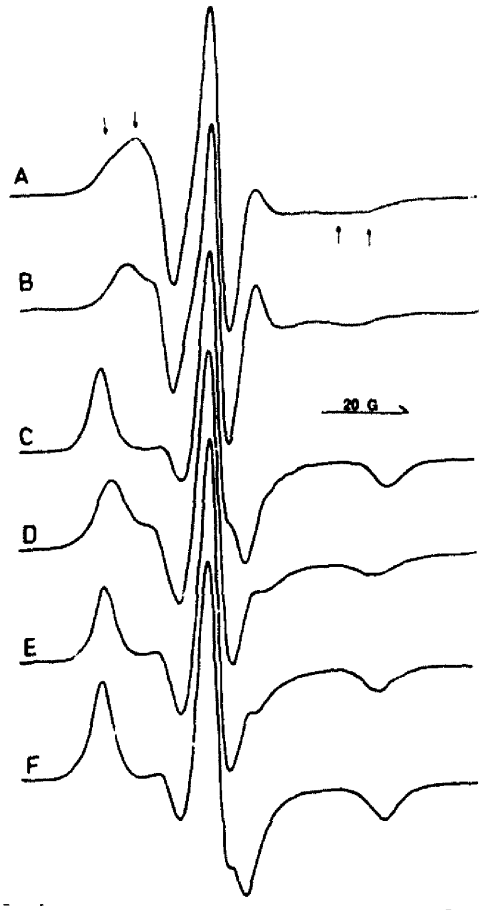


Fig. 6. ESR spectra of (A) 16-MeS-SL in 1,2-DPPC at 9°C (vertical arrows indicate the two components in the spectrum referred to in the text); (B) 16-MeS-SL in DHPC at 9°C (the spectrum is similar in 1,3-DPPC); (C) PG-SL in DPPG/PMB (5:1, molar ratio) at 9°C; (D) PG-SL in DPPG at 9°C; (E) 5-S-SL at 9°C in DHPC; and (F) 5-S-SL at 9°C in 1,2-DPPC. Spectra in (A–D) and (E, F) are plotted normalized to the same center peak height. All samples were heated to above the phase transition temperature before measuring the spectra.

also motionally restricted with similar $T_{max}$ values in DPPG/PMB and 1,2-DPPC/glycerol (Table I). However, like 16-S-SL, 16-MeS-SL is not significantly restricted in DHPC or 1,3-DPPC; the $T_{max}$ value is only slightly greater than that in the non-interdigitated 1,2-DPPC. There is one difference in the behavior of this spin label in these interdigitated bilayers from that in non-interdigitated 1,2-DPPC, which is consistent with the differences in structure, but which would probably not be very useful in diagnosing their structures. This spin label has two components in 1,2-DPPC at 9°C, as shown in Fig. 6A, while it has only one component in the interdigitated bilayers of DHPC and 1,3-DPPC (Fig. 6B). The cause of the two components in 1,2-DPPC is probably orientation of this less polar spin label in the bilayer in two directions, one with the ester group near the bilayer/aqueous interface, and the other with the spin label group near the bilayer/aqueous interface and the ester group in the center of the bilayer. The former gives a component characteristic of greater motion than the latter. In the interdigitated bilayer, however, there is only one way in which this spin label can be oriented. Thus, observation of a single component spectrum for this spin label is consistent with an interdigitated bilayer structure even if the spin label is not significantly more motionally restricted than in a non-interdigitated bilayer.

Although PG-SL is more motionally restricted than the single chain spin labels in the interdigitated bilayers of 1,3-DPPC, DHPC or 1,2-DPPC with 100 mg/ml ethanol, the difference in $T_{max}$ values for PG-SL at low temperatures in interdigitated and non-interdigitated bilayers is less than 2 G. In contrast, for interdigitated DPPG-PMB at 9°C, the $T_{max}$ value of PG-SL is 3 G more than in non-interdigitated DPPG (Fig. 6C, D). The fact that the difference in $T_{max}$ values of 16 MeS-SL, 16-S-SL, and PG-SL in the non-interdigitated bilayer of 1,2-DPPC from the interdigitated bilayers of DHPC, 1,3-DPPC, or 1,2-DPPC-ethanol is not as great as the difference from the interdigitated bilayers of 1,2-DPPC-glycerol, DPPG-PMB, or 18:10PC, suggests that the former interdigitated lipid systems may be less closely packed and allow the probe greater freedom of motion near the bilayer/aqueous interface than the latter.

In order to compare the packing and structure of these lipids near the apolar/polar interface, we used 5-S-SL and H-TEMPO. These probes are expected to have relatively similar behavior in interdigitated and non-interdigitated bilayers since their location in the bilayer relative to the apolar/polar interface is similar in both cases. If differences are observed it indicates that there are differences in the packing of the lipids near this interface in the two types of bilayer. Such differences in the packing of various lipids in interdigitated bilayers would be expected to also affect the motion of spin labels containing 16-S-SL. Both 5-S-SL and H-TEMPO are relatively motionally restricted in non-interdigitated gel phase bilayers with $T_{max}$ values of 30–32 G. However, they have somewhat larger $T_{max}$ values in the interdigitated bilayers of 1,2-DPPC/glycerol and DPPG/PMB than in non-interdigitated bilayers (Table I). In the mixed interdigitated bilayer of 18:10PC these probes have similar $T_{max}$ values to 1,2-DPPC. In contrast, both have somewhat lower $T_{max}$ values in the interdigitated bilayers of DHPC and 1,2-DPPC-ethanol (100 mg/ml) than in non-interdigitated bilayers. This is true at all temperatures below the transition temperature. The spectra of 5-S-SL in DHPC and 1,2-DPPC at 9°C, are compared in Fig. 6E and F, respectively. H-TEMPO is also less motionally restricted in the interdigitated bilayer of 1,3-DPPC than in 1,2-DPPC but 5-S-SL has similar motion in these two lipids.

Thus those interdigitated bilayers which cause the greatest motional restriction of 16-S-SL, 16-MeS-SL, and PG-SL allow less freedom of motion to 5-S-SL or H-TEMPO near the apolar-polar interface than a non-interdigitated bilayer. This lower freedom of motion might be due to greater order or closer packing of the lipid in the interdigitated bilayers compared to the non-interdigitated bilayers studied or, in the case of PMB, to penetration of hydrophobic amino acid side chains of the peptide partway into the region of the bilayer near the apolar/polar interface. Those interdigitated bilayers which cause less restriction of 16-S-SL and similar spin labels are less ordered or less closely packed near the apolar/polar interface than a non-interdigitated bilayer.

## Discussion

The main difference between interdigitated and non-interdigitated gel phase bilayers, which can be exploited for determination of their structure using spin labels, is that the former have a much less steep fluidity gradient. The present study also reveals that the motion of PG-SL in the interdigitated bilayer is less temperature dependent than in the non-interdigitated bilayer. These differences apply to the fully interdigitated bilayers formed by symmetric chain lipids and the mixed, triple-chain bilayers formed by asymmetric chain lipids. (However, partially interdigitated bilayers probably also have a relatively steep fluidity gradient and may be difficult to detect with spin labels.) Thus a long chain amphiphilic probe in which the nitroxide group is near the terminal methyl should experience relatively similar freedom of motion in fully or mixed interdigitated bilayers as one in which the nitroxide group is close to the polar head group. Indeed, this was shown to be the case in earlier studies for 1,2-DPPC/glycerol, DPPG/PMB, and asymmetric chain length PCs [24,25] and in the present study for 1,3-DPPC, DHPC, and 1,2-DPPC/ethanol. Observation of similar behavior in vesicles of DPPG with myelin basic protein or polymyxin B nonapeptide, and asymmetric chain length species of cerebroside sulfate allowed the prediction that these also can form interdigitated bilayers [3,21,26].

If the non-interdigitated bilayer is highly ordered it may be difficult to distinguish a difference from the interdigitated bilayer at low temperatures. However, the motion of probes with the nitroxide near the terminal methyl is less dependent on temperature in interdigitated bilayers than in non-interdigitated bilayers. Hence the difference should increase as the temperature is increased as long as the interdigitated bilayer does not transform to a non-interdigitated bilayer. Thus although PG-SL is only a little more ordered in the interdigitated bilayers of DHPC, 1,2-DPPC/ethanol, and 1,3-DPPC than in the non-interdigitated bilayer of 1,2-DPPC at low temperatures, the high degree of order is retained in the interdigitated bilayers as the temperature is increased, but not in the non-interdigitated bilayer. A significant difference between the interdigitated and non-interdigitated bilayers can then be detected. Conversely, if the interdigitated bilayer is disordered or loosely packed, it may also be difficult to detect a difference from non-interdigitated bilayers at low temperatures. However, the fluidity gradient should still be less steep in the interdigitated bilayer than in the non-interdigitated bilayer. Thus if a probe labeled near the terminal methyl of the chain experiences greater freedom of motion in some interdigitated bilayers, then so should a probe labeled closer to the head group. Indeed, this was found to be the case for the interdigitated bilayers of 1,3-DPPC, 1,2-DPPC/ethanol and especially DHPC.

The nitroxide group on the 16th carbon of one chain of PG-SL is more ordered than when on a free fatty acid chain in these latter interdigitated bilayers and also in non-interdigitated bilayers. This is probably because the vertical position of the lipid spin label in the bilayer may be different from that of the fatty acid spin label. The latter may be embedded less deeply in the bilayer so that the carboxyl group can interact with the phosphate of the head group of lipids in the bilayer [46]. The fatty acid chain length of the spin labels used is longer than that of the C-16 lipid bilayer systems studied, and thus even in a non-interdigitated bilayer it may interdigitate itself to some extent into the other side of the bilayer. This probably occurs more for the lipid spin label than the fatty acid spin label. A lipid spin label which is identical to the lipid system being studied, in both head group, backbone, and chain length, would of course be best for studying the structure of a lipid bilayer. A long fatty acid chain length sphingolipid spin label has been designed to monitor interdigitation of the long fatty acid chain into the other side of a non-interdigitated bilayer of symmetric chain length lipids [40].

However, the spin labels related to 16-S-SL used in this and previous studies are able to detect a difference between the interdigitated and non-interdigitated gel phase bilayers in all cases. By using suitable temperatures and at least one of these spin labels, the difference is sufficiently clear-cut to be of diagnostic value. As with any spectroscopic technique, caution must be exercised when using spin labels to diagnose interdigitation in lipid bilayers of unknown structure. Other phenomena or agents may be discovered which can cause similar effects in the absence of interdigitation. The only agents known of at present which have a similar effect on the motion of spin labels containing 16-S-SL are membrane-spanning intrinsic proteins. However, the motional restriction which they cause can be distinguished from that of interdigitation because the former also occurs in the liquid-crystalline phase. Even

if some kind of interdigitation occurred in the liquid-crystalline phase it would cause much less motional restriction of the spin labels than that which occurs in the gel phase or that caused by intrinsic proteins. Thus with occasional back-up by X-ray diffraction and in the absence of intrinsic proteins, we suggest that the spin label technique will prove useful to diagnose interdigitation of lipid bilayers with a good degree of reliability, if a motionally restricted spectrum is observed. However, if the interdigitated bilayer is disordered, then it may not be possible to diagnose its structure using spin labels. The spin label technique can also be invaluable for more detailed studies of known interdigitated bilayers which would be time- and material-consuming if done by X-ray diffraction.

Other spectroscopic techniques are also being used to study interdigitated lipid bilayers. Raman spectroscopy has detected a decrease in the $I_{2850}/I_{2880}$ peak height intensity ratio in the interdigitated bilayers of 1,2-DPPC/glycerol [28], DHPC [37], DPPG/PMB [29], and asymmetric chain length lipids [16]. This is attributed to increased chain-chain lateral interactions in the interdigitated bilayer. However, a similar decrease in this ratio occurs when polylysine is added to DPPG; yet X-ray diffraction shows that interdigitation does not occur [41]. Thus caution is required when using this technique also. Differences between the interdigitated bilayers of DHPC and 1,2-DPPC and non-interdigitated 1,2-DPPC can also be detected by high-pressure infrared spectroscopy at pressures of about 3 kbar or higher [30,31]. However, pressure itself induces interdigitation if the cross-sectional area occupied per hydrocarbon chain is less in the interdigitated bilayer than in the phase adopted by the lipid at atmospheric pressure [13,42]. This may often be the case and hence this technique may not be useful for an understanding of the structure of unknown lipid phases at atmospheric pressure.

The present study also provides some new information about these interdigitated bilayers. The results indicate that DHPC, 1,3-DPPC, and 1,2-DPPC/ethanol form more disordered or less closely packed interdigitated bilayers than those formed by 1,2-DPPC/glycerol, DPPG/PMB, and asymmetric chain length lipids, with DHPC being the most different. $^{14}N$- and $^{31}P$-NMR studies [2,43] showed that DHPC has fast axial diffusion down to $-20°C$, in contrast to 1,2-DPPC, while an infrared spectroscopy study of 1,3-DPPC at atmospheric pressure indicated that it has high mobility about its long axis [44]. High pressure infrared spectroscopy indicated that there is a greater difference between 1,2-DPPC and 1,3-DPPC than between 1,2-DPPC and DHPC [30], also suggesting differences in the structure of these interdigitated bilayers. Our results on 1,3-DPPC suggest, in addition, that once the crystalline phase has undergone its transition to the interdigitated gel phase, this phase exists at all temperatures from 4°C up to the gel to liquid-crystalline phase transition temperature and that the transition of the interdigitated gel phase to the liquid-crystalline phase is reversible. Slow cooling, however, allows the crystalline phase to reform. The results also indicate that 1,2-DPPC/ethanol goes into its interdigitated gel phase soon after the transition from the liquid-crystalline phase is complete.

## Acknowledgements

This study was supported by an operating grant and Scientist Award to J.M.B. from the Medical Research Council of Canada. We thank Dr. J.T. Mason for a generous gift of 18 : 10PC.

## References

1 Serrallach E.N., Dijkman, R., De Haas, G.H. and Shipley, G.G. (1983) J. Mol. Biol. 170, 155–174.
2 Ruocco, M.J., Siminovitch, D.J. and Griffin, R.G. (1985) Biochemistry 24, 2406–2411.
3 Boggs, J.M., Stamp. D. and Moscarello, M.A. (1981) Biochemistry 20, 6066–6072.
4 Tirrell, D.A., Turek, A.B., Wilkinson, D.A. and McIntosh, T.J. (1985) Macromolecules 18, 1513–1515.
5 Ranck, J.L. and Tocanne, J.G. (1982) FEBS Lett. 143, 171–174.
6 Ranck, J.L. and Tocanne, J.G. (1982) FEBS Lett. 143, 175–178.
7 McDaniel, R.V., McIntosh, T.J. and Simon, S.A. (1983) Biochim. Biophys. Acta 731, 97–108.
8 McIntosh, T.J., McDaniel, R.V. and Simon, S.A. (1983) Biochim. Biophys. Acta 731, 109–114.
9 Theretz, A., Ranck, J.L. and Tocanne, J.F. (1983) Biochim. Biophys. Acta 732, 499–508.
10 Simon, S.A. and McIntosh, T.J. (1984) Biochim. Biophys. Acta 773, 169–172.
11 Wilkinson, D.A., Tirrell, D.A., Turek, A.B. and McIntosh, T.J. (1987) Biochim. Biophys. Acta 905, 447–453.
12 Cunningham, B.A. and Lis, L.J. (1986) Biochim. Biophys. Acta 861, 237–242.
13 Braganza, L.F. and Worcester, D.L. (1986) Biochemistry 25, 2591–2596.
14 Hui, S.W., Mason, J.T. and Huang, C. (1984) Biochemistry 23, 5570–5577.
15 McIntosh, T.J., Simon, S.A., Ellington, Jr., J.C. and Porter, N.A. (1984) Biochemistry 23, 4038–4044.
16 Levin, I.W., Thompson, T.E., Barenholz, Y. and Huang, C. (1985) Biochemistry 24, 6282–6286.
17 Mattai, J., Witzke, N.M., Bittman, R. and Shipley, G.G. (1987) Biochemistry 26, 623–633
18 Schmidt, C.F., Barenholz, Y., Huang, C. and Thompson, T.E. (1978) Nature 271, 775–777.
19 Mattai, J., Sripada, P.K. and Shipley, G.G. (1987) Biochemistry 26, 3287–3297.
20 Reed, R.A. and Shipley, G.G. (1987) Biochim. Biophys. Acta 896, 153–164.
21 Boggs, J.M., Koshy, K.M. and Rangaraj, G. (1988) Biochim. Biophys. Acta 938, 373–385.
22 Vincent, J.M. and Skoulios, A.E. (1966) Acta Cryst. 20, 432–440.
23 Ranck, J.L., Keira, T. and Luzzatti, V. (1977) Biochim. Biophys. Acta 488, 432–441.

24 Boggs, J.M. and Rangaraj, G. (1985) Biochim. Biophys. Acta 816, 221–233.
25 Boggs, J.M. and Mason, J.T. (1986) Biochim. Biophys. Acta 863, 231–242.
26 Kubesch, P., Boggs, J.M., Luciano, L., Maass, G. and Tümmler, B. (1987) Biochemistry 26, 2139–2149.
27 Huang, C., Mason, J.T. and Levin, I.W. (1983) Biochemistry 22, 2775–2780.
28 O'Leary, T.J. and Levin, I.W. (1984) Biochim. Biophys. Acta 776, 185–189.
29 Babin, Y., D'Amour, J., Pigeon, M. and Pezolet, M. (1987) Biochim. Biophys. Acta 903, 78–88.
30 Siminovitch, D.J., Wong, P.T.T. and Mantsch, H.H. (1987) Biochim. Biophys. Acta 900, 163–167.
31 Siminovitch, D.J., Wong, P.T.T. and Mantsch, H.H. (1987) Biophys. J. 51, 465–473.
32 Nambi, P., Rowe, E.S. and McIntosh, T.J. (1988) Biophys. J. 53, 122a.
33 Hubbell, W.L. and McConnell, H.M. (1971) J. Am. Chem. Soc. 93, 314–326
34 Davis, J.H. (1979) Biophys. J. 27, 339–358.
35 Jost, P.C., Griffith, O.H., Capaldi, R.A and Vanderkooi, G. (1973) Proc Natl. Acad. Sci. USA 70, 4756–4763.
36 Kim, J.T., Mattai, J. and Shipley, G.G. (1987) Biochemistry 26, 6592–6598.
37 Levin, I.W., Kelhn, E. and Harris, W.C. (1985) Biochim. Biophys. Acta 820, 40–47.
38 Rowe, E.S. (1983) Biochemistry 22, 3299–3305.
39 Rowe, E.S. (1985) Biochim. Biophys. Acta 813, 321–330.
40 Grant, C.W.M., Mehlhorn, I.E., Florio, E. and Barber, K.R. (1987) Biochim Biophys. Acta 902, 169–177.
41 Carrier, D. and Pezolet, M. (1986) Biochemistry 25, 4167–4174.
42 Wong, P.T.T. and Mantsch, H.H. (1986) J. Raman Spectrosc. 17, 335–340.
43 Siminovitch, D.J., Jeffrey, K.R. and Eibl, H. (1983) Biochim. Biophys. Acta 727, 122–134.
44 Dluhy, R.A., Chowdhry, B.Z. and Cameron, D.G. (1985) Biochim. Biophys. Acta 821, 437–444.
45 Marsh, D. and Watts, A. (1982) in Lipid-Protein Interactions, Vol. 2, (Jost, P.C. and Griffith, O.H., eds.), pp. 53–126, Wiley-Interscience, New York.
46 Boggs, J.M., Rangaraj, G. and Koshy, K.M. (1986) Chem. Phys. Lipids 40, 23–34.
47 Freed, J.F. (1976) in Spin Labeling, Theory and Applications (Berliner, L.J., ed.), pp. 53–132, Academic Press, New York.